Determining characteristic morphological wavelengths for Venus using Baltis Vallis.

J. W. Conrad[1], F. Nimmo[2]

[1]NASA Marshall Space Flight Center, Huntsville, AL, USA (jack.w.conrad@nasa.gov).
[2]University of California Santa Cruz, Santa Cruz, CA, USA.

Key Points:

- We show that the topography of the longest channel on Venus was modified along most of its length, depending on its source location.
- Fourier analysis of the channel's topography reveals three sets of dominant wavelengths, ~110-235 km, ~640±25 km and ~3500±1200 km.
- The longest of these can be linked to the wavelength of crustal dynamic uplift by mantle plumes, a useful value for Venus interior models.

Abstract

One of Venus' most enigmatic landforms is Baltis Vallis, the longest observed channel on the surface (~7000 km long). Topographic conformity analysis shows that Baltis Vallis was modified over most of its observed wavelengths. Since the source location of Baltis Vallis is not well constrained, we analyze in both flow directions. For the commonly used northern source, topography across all wavelengths appears to be created after Baltis Vallis. However, for the southern source, topographic components with wavelengths longer than ~1900 km might have previously existed. Fourier analysis reveals three characteristic wavelengths, ~110-235 km, ~640±25 km and ~3500±1200 km. The shortest corresponds to deformation belts that cross Venus' low plains, while the medium currently lacks an explanation. The longest is plausibly associated with the wavelength of dynamic uplift of the crust by mantle plumes. Higher resolution observations provided by the VERITAS mission can help resolve the source location of Baltis Vallis.

Plain Language Summary

Venus' surface is covered in a plethora of strange landforms, at least from the perspective of Earth. One of the longest is an about 7000 km channel named Baltis Vallis, comparable to the Amazon and Nile rivers, but instead likely formed by volcanic processes. Baltis Vallis serves as a unique opportunity on Venus due to its length. The channel recorded the surface altering processes in its topography, but we first check if the channel retained topography from when it initially formed. We find that processes up to about 1900 km in width that altered the topography of Baltis Vallis must have happened after the channel was carved, but above that it depends on the channel source location. In the northern source case, Baltis Vallis was altered over its entire length. When we analyze the topography of the channel, 3 length-scales are found to be overrepresented in the topography. The shorter length-scales correspond to the thin mountain range-like features that cross Venus' low plains, while the medium

value currently lacks an explanation. The longest wavelength is plausibly associated with uplift of the crust by mantle plumes and this value will be useful when creating models of Venus' interior.

1. Introduction

The surface of Venus is dominated by volcanic and tectonic processes, with a large portion of the surface covered in volcanic plains, wrinkle ridges, and deformation belts. However, there are some rare features which are difficult to explain with the limited information obtained from past spacecraft missions, including features like canali (Komatsu & Baker, 1994) and tesserae valleys (Khawja et al., 2020), that putatively need erosional processes to create them. The material that eroded these features must have flowed along the maximum downhill gradient. If the present-day topography does not conform to this expectation, that is evidence of post-emplacement deformation of the surface. Canali, sinuous and putatively erosional channels, might serve as useful tools as we attempt to understand the global and local processes that have modified topography across Venus. Canali were likely formed either by exotic magmas (Komatsu & Baker, 1994) or water (Jones & Pickering, 2003). The exact erosional medium, while important to the formation timing of these features, has little bearing on their usefulness for this study. The more important aspect of canali in this context is the length of their channels, which are thought to have formed in less than ~100 years (Kargel et al., 1994). While most observed canali are relatively short (tens to hundreds km), a particular canale is comparable in its dimensions to Earth's longest rivers. That canale, Baltis Vallis (BV), is the longest of the canali at about 7000 km in length, roughly equivalent to the Nile or Amazon rivers on Earth. This extreme length of BV has allowed it to be sensitive to processes across a broad range of wavelengths.

Beyond BV's existence as an erosional landform with an exceptional length on a planet with a surface temperature hotter than the melting point of lead, it also has a complex stratigraphical and formation history. If we follow Baker et al. (1992)'s proposed placements of BV's source at a volcanic vent near the northern end (44.5° N, 185° E) and terminus at the southern end, the canale seemingly flowed uphill over most of its length (Figure 1). This apparent uphill "flow" is a signal of the age of the feature: it must have been emplaced when the path of BV represented the maximum downhill gradient from the canale source, then later processes like tectonic uplift and deformation altered the topographic profile. We do not find Baker et al. (1992)'s assignment of a "nearby" (~300 km) circular volcanic construct as the northern source location to be very convincing, since there are no obvious flows that cover the intervening region. On the other hand, there are no published observations that point towards the contrary (southern) source, although there is a possible lemniscate loop (see Komar, 1984) at 160.75° E, 42.12° N that implies a south-to-north flow direction. We will present results in the following sections for both possible BV source placements (northern and southern).

The ability of BV to act as a recorder for the tectonic uplift history of Alta

Regio and Rusalka Planitia is the focus of our study, especially if it can be used to determine the characteristic wavelengths of general tectonic uplift or specific features like deformation belt formation. Similar studies have used topographic profiles on other worlds in our solar system to obtain characteristic wavelengths (e.g., Rhea; Nimmo et al., 2010, and Pluto and Charon; Conrad et al., 2021). Venus itself has also been studied in terms of its topographic spectral characteristics (e.g., Sharpton & Head, 1985; James et al., 2013). However, except for one abstract (Jindal et al., 2018) or statements made without explicit numerical analysis (Baker et al., 1992) the two have not been brought together in the context of canali on Venus.

Our first step is to understand if significant topographic information from BV's initial state as a drainage system remains. If so, our topographic analysis will be biased by that precursor information and give us information about processes that occurred before the formation of BV. We thus need a method to quantify how similar BV topography is to drainage systems on other worlds. This will be done using a technique developed for comparing drainage systems on Earth and Mars (Black et al., 2017). Then we will analyze BV using a topographic power spectrum technique to determine characteristic wavelengths for profile-altering processes.

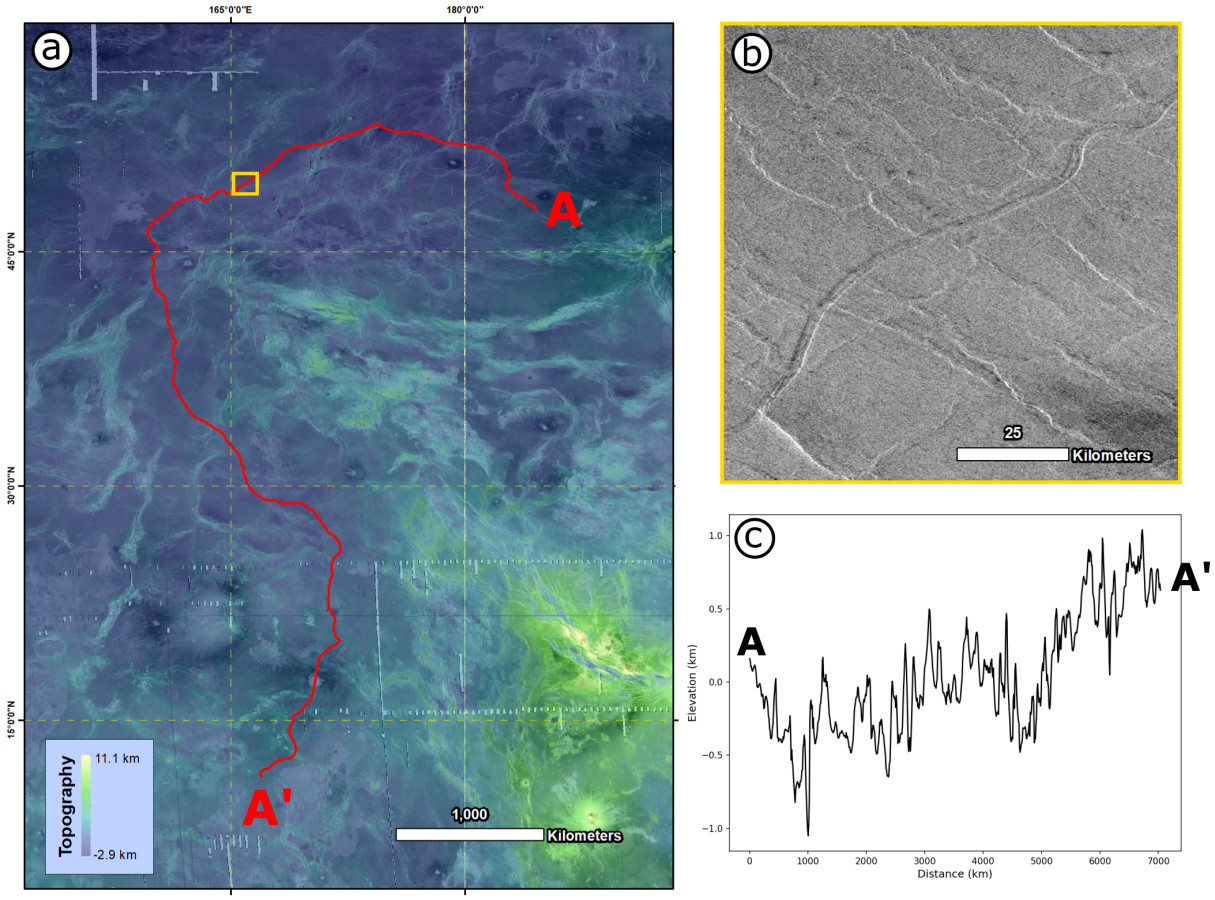

Figure 1: Panel a. Map of Baltis Vallis in Atla Regio. The standard proposed source of BV is at location A, and the end is at A' (Baker et al., 1992). Notice how BV avoids the topographic high to its southeast, but cuts through shorter wavelength topography. Panel b. A close-in look at the canale at 49.25 ° north, 165.74 ° east. The width of BV is consistent over its whole length (~2 km; Oshigami & Namiki, 2007). Panel c. Topographic profile of BV with labels that correspond to the map locations. Vertical exaggeration is ~2500x.

2. Topographic Conformity

While the modern-day BV topographic profile does not conform to a typical fluvial system (Figure 1), we want to assess the extent to which the canale's topography has been modified by post-formation processes over a broad range of wavelengths. If we follow Baker et al. (1992)'s interpretation of BV's emplacement, the profile has been tilted along its longest wavelength. In addition, the canale's profile might also contain emplacement information at shorter wavelengths. We would like to determine if the initial emplacement information still

exists as an observable factor in the topography and if so at which length scales it competes with post-emplacement processes. To determine this, we will consider two metrics from Black et al. (2017) for comparing the "drainage" pattern of fluvial systems to topography over a wide range of wavelengths. The two metrics, downhill percentage ($\%d$) and the conformity factor (Λ), were used by Black et al. to analyze the drainage systems of the Earth, Mars, and Titan. The metric $\%d$ is equal to the proportion of points along the path of drainage that are at a higher elevation than the next point downstream. Λ is defined as Λ = median(cos( )), where is the angle between the system's drainage direction and the direction of the maximum negative topographic gradient. These metrics can be thought as the degree to which the vertical and horizontal gradients of the profile align with the topography. This analysis is done over a range of wavelengths by generating topography from spherical harmonic coefficients. Topography is incrementally built up with sets of coefficients, with higher degree (shorter wavelength) coefficients added onto the topography. With each new maximum degree (l_{max}), we sample a BV profile and calculate the $\%d$ and Λ from that profile and the surrounding topography. For Venus, these coefficients are calculated from Ford and Pettengill (1992)'s Doppler-sharpened radar topography. We compared the coefficients to Wieczorek et al. (2015)'s Venus topographic coefficients and found that for the degree range we are using in our analysis (up to degree 90) there is no significant difference in the results.

Black et al. found that for fluvial systems on Earth, Mars, and Titan, as topography is built up using higher l_{max} spherical harmonic expansions, both metrics trend towards specific values: 100% for $\%d$ and 1 for Λ. This is the expected result when the drainage systems are formed concurrently or after tectonic uplift and can conform rapidly to contemporary topography. In addition to the high l_{max} asymptotic behavior, there are also signatures of the relative timing of fluvial and tectonic processes in the behavior of the metrics at lower degrees/longer wavelength. A signature of this is present in how the Earth's metrics lag Mars and Titan's at lower l_{max}. This terrestrial signature is expected for drainage systems that are still evolving in response to ongoing tectonic uplift. Both metric behaviors, the short wavelength asymptotic behavior and long wavelength initial trend, should be considered for BV as the combination of those two behaviors tells us at which wavelengths the canale has experienced a measurable degree of post-emplacement deformation.

We use the metric analysis on the topography of BV and compare it to Black et al.'s Earth and Mars results. However, since BV is a singular flow feature compared to the numerous rivers and channels that Black et al. (2017) used for Earth and Mars, we need to beware of possible biases in our results. The sources of bias we are most concerned with arise from using a singular, geographically constrained profile. To study this, we use topographic profiles of pseudo-BVs made with synthetic topography to calculate the metric ranges expected from a single profile. The synthetic topography is generated using randomized spherical harmonic coefficients that conform to a power spectrum with the same shape as Venus' (Wieczorek et al., 2015). We keep the degree 0 term (i.e., the mean

radius) consistent with Venus, but vary the typically constant degree 1 and 2 terms as they contribute significantly to the observed topography even above the geoid (Wieczorek et al., 2015). Pseudo-BVs are placed at the exact same location with the same extent as the real BV. While the processes that altered the real BV are not random, in the context of the drainage metrics long term tectonic processes that occur after the drainage system is already emplaced and unable to adapt should produce results that are equivalent to random topography. Using these synthetic profiles allows us to understand the range of metric values that we would expect for a feature whose modern topographic information is dominated by post-emplacement, non-fluvial processes.

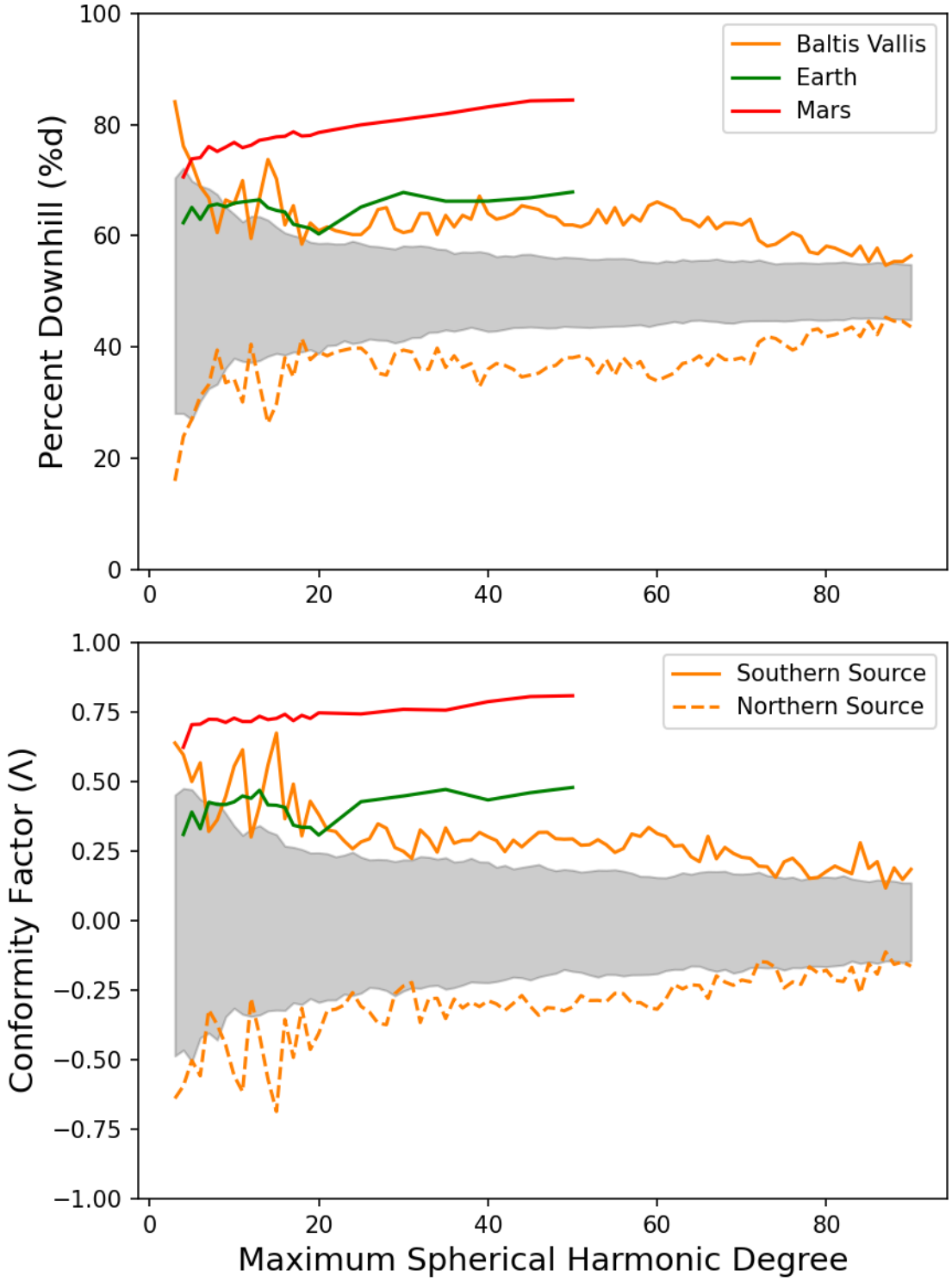
Percent Downhill (%d)
Baltis Vallis
Earth
Mars
Conformity Factor (Λ)
Southern Source
Northern Source
Maximum Spherical Harmonic Degree

Figure 2: Top: Percent downhill values for Earth (green), Mars (red), Baltis Vallis (orange), and synthetic versions of Baltis Vallis (gray envelope). Solid line is the southern source curve, and the dashed line is the northern source supported by Baker et al. (1992). Bottom: Conformity factor with the same set of sources. Earth and Mars data are from Black et al. (2017). The behavior of BV is more akin to the randomized topography than that of Earth or Mars.

The grey regions in Figure 2 represents the metric results of our 100 pseudo-BVs made from synthetic spherical harmonic coefficients. The standard deviation of those 100 profiles is plotted as an envelope which allows us to observe the trends in the metric ranges expected from long term tectonic processes. For $\%d$ the synthetic profiles narrow in on ~49.9±5.0% at large maximum degrees. The synthetic group's behavior at short wavelengths is divergent from Black et al. (2017)'s results for Earth and Mars. The short-wavelength synthetic behaviour arises from the fact that with random topography the profile should go uphill about the same amount as it goes downhill (i.e., $\%d \sim 50\%$). Based on the synthetic envelope, we should expect a profile that has had tectonic processes alter the initial emplacement topography start with a wide possible range of long wavelength $\%d$ metric values and then trend towards ~50% with the addition of shorter wavelength topography.

When we consider the synthetic group's conformity factor results, there are many similarities compared with the $\%d$ results. The mean Λ at our highest l_{max} is approximately zero, as expected (incoherent topography should point perpendicular as a median). The shape of the Λ envelope is also similar to the results for $\%d$, although it does not narrow as quickly at high l_{max}. Λ could be more volatile compared to $\%d$ as it is sensitive to an extra degree of freedom (1-D versus 2-D). The similar shapes of the $\%d$ and Λ envelopes falls in line with what Black et al. found for the worlds they studied, where the two metrics generally have similar characteristics and convey the same information. This is to be expected for any surficial fluvial system that follows the topographic structure, as the next point downhill in the profile should also be the point along the direction of the maximum gradient.

For the BV curves (orange), we plot up the results for the two possible source locations. While Baker et al. (1992) support a northern source location, we plot results for both possible source locations. This allows for the possibility of new interpretations that may be provided by *VERITAS* spacecraft observations (see Conclusions). As we would expect, the two curves end up being mirrored across the 50% and 0 values of the metrics. Each curve has different implications for how we interpret the results of the next section so we will detail them individually.

When the BV source is placed at Baker et al. (1992)'s proposed location (Fig. 3, dashed orange lines), the $\%d$ metric starts at a low percentage due to the profile's long wavelength upslope tilt (~15% at l_{max}=3) and rapidly trends upwards while staying below the pseudo-BV metrics. The Λ curve behaves similarly to the $\%d$ curve, although the initial rate at which the curve trends towards the high l_{max}

asymptote is lower. A clear issue with using a single canale can be observed in the spikiness of BV's Λ curve, as a single profile's topography can change wildly with the addition of a single degree's worth of information given the higher topographic power at lower spherical harmonic degrees. Both metrics are clearly separate from Black et al.'s values, but the BV metrics have a similar shape except offset downwards by ~30-40% and ~-1. This could be explained with a BV that initially had $\%d$ and Λ metrics more like Mars before the process that created the observed tilt lowered the metrics across all wavelengths.

For both northern source BV curves, they typically remain outside the synthetic standard deviation envelope, but on the other side of the envelope compared to Earth and Mars' curves. Both of the metrics also are moving towards an asymptotic value of ~50%/0, corresponding to the high l_{max} behavior of the pseudo-BV metrics, but still remain outside the synthetic envelope at $l_{max} = 90$. The most likely explanation for how this metric curve shape is formed is that the long-wavelength tilt along BV (Figure 1) pulled the curves down to values denoting a dominant uphill signal, while shorter wavelength topography-generating processes are pushing the curves towards the asymptotic (random) values. The comparison of BV metric values to the synthetic metric envelope and Black et al.'s Earth and Mars values suggests that the topographic information left from the original fluvial profile has been overwritten by subsequent processes over the entire observed wavelength range. If we consider the full profile tilt as well, there have been processes that altered the topographic profile which are much wider than the profile itself and thus will not be captured by our topographic power spectra analysis in the next section.

As for the southern source case curve (Fig. 3, solid orange line), both metrics at low l_{max} start at relatively high values, even compared to Mars. Yet they trend in an opposite manner to both Earth and Mars, with rapidly decreasing conformity to topography as shorter wavelength degrees are added. This behavior is unexpected. What it implies is that the longest wavelengths of the BV profile contain information about the pre-formation topography, while the shorter-wavelength topography was added after emplacement. Just as in the northern source case, the source-to-terminus difference in topography is difficult for shorter wavelength topography to completely erase. We set the degree l_{max} at which the dominance of the long-wavelength topography ends to be 20 (corresponding to a wavelength of ~1900 km), where both metrics for this interpretation drop below Earth's metric values. For longer-wavelength features, we cannot constrain the timing to postdate the formation of BV, limiting its use to further constrain Venus' internal and surface processes.

In either source location scenario, BV probably formed over a relatively short timescale (~1 to 100 yrs; Kargel et al., 1994) and was not responsive to topographic changes during its formation. Then later processes came into play that altered the topography in the region including BV, producing topography across a broad range of wavelengths that left the topographic profile that we observe today. The main difference between the two source location interpre-

tations is the long wavelength features ($l_{max} < 20$): in the case of a southern source, whether they existed prior to emplacement of the canale is ambiguous, while in the case of a northern source they must have been generated subsequent to BV's emplacement. These results give us confidence that if we perform the topographic power spectrum analysis, any clear signal in the results is a signal of tectonic processes that occurred after the formation of BV for the northern source or if the wavelength is less than ~1900 km ($l_{max} > 20$) for the southern source.

3. Topographic Power Spectra

The topographic power spectrum is a powerful tool used to analyze topography. The spectrum allows us to quantify topographic roughness as a function of wavelength (Shepard et al., 2001; Araki et al., 2009; Nimmo et al., 2010; Ermakov et al., 2018). This tool has been used on a wide range of worlds, including Venus (e.g., Bills & Kobrick, 1985), to understand those worlds' global topographic roughnesses. To obtain Baltis Vallis' power spectrum, we first calculate the discrete Fourier transform for the profile. For a set of evenly spaced topographic observations h_i, the discrete Fourier transform is (Press, 1992):

$$H_j = \sum_{i=0}^{N-1} h_i e^{\frac{2\pi i j \sqrt{-1}}{N}} \quad (1)$$

where *i, j* are integers, N is the number of points in our topographic profile, and the wavenumber k associated with H_j is given by $k = 2$ *(j-1)*$/L$, where L is the total length of the topographic profile. We process the profile to have consistently spaced gridding and de-trend the profile such that the endpoints are set to zero. While this removes the full profile's tilt to reduce ringing in the power spectrum, the wavelength of the tilting process is longer than the profile itself and likely is associated with the creation of Alta Regio's topographic high to the south and west of the canale. After these corrections, we can calculate H_j from Equation 1, which we then use to calculate the power at each wavelength as ${H_j}^2/N^2$. The results for the power found over the range of possible wavelengths can be found in Figure 3.

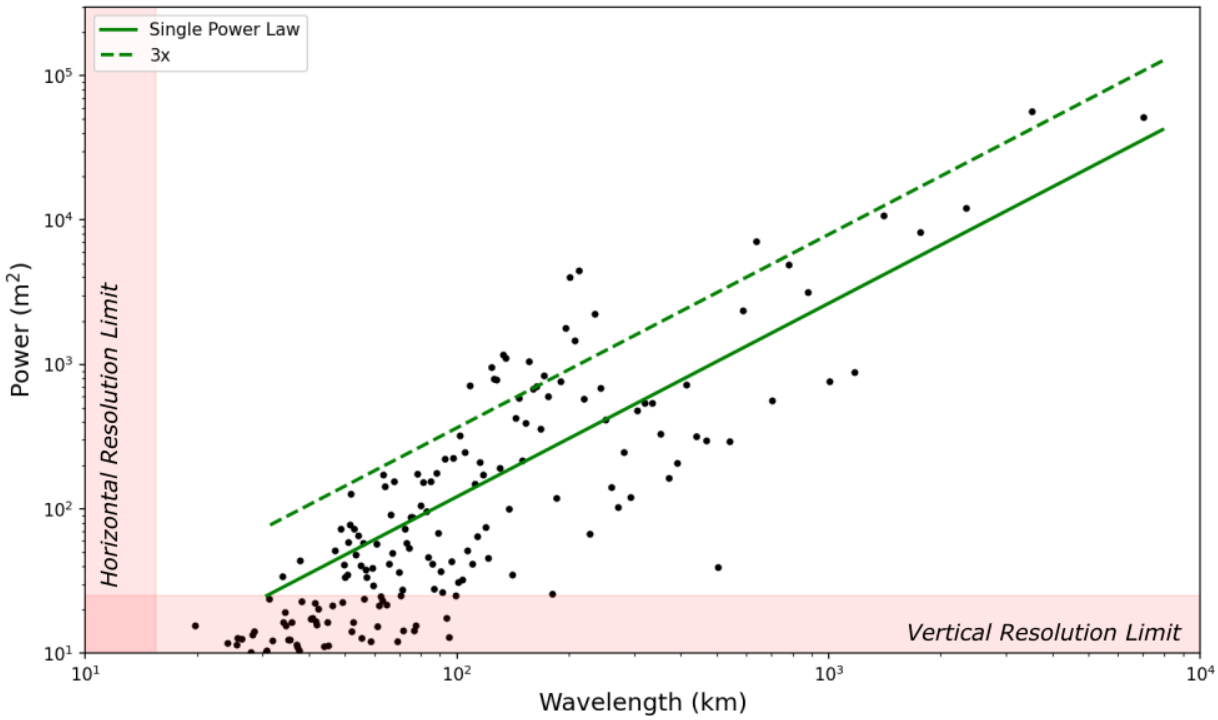

Figure 3: Power distribution spectrum of Baltis Vallis with the best single power-law fit plotted in green. We also plot power-law slope that is a factor of 3 higher in value (approximately 0.5 units higher logarithmically) to showcase outlying points above the primary distribution. The red shaded regions represent the resolution limits to the topographic data.

When plotted on a log-log scale, topographic power spectra as a function of wavelength typically conform to a slope of ~2 (Ermakov et al., 2018). We apply a single slope power-law fit to the data that lies above the resolution limits (see Wieczorek, 2015 for a more detailed discussion). The BV spectrum fit has a slope of ~1.34 and is best fitted by a single power-law when we compare it to the best multi-slope and polynomial fits with a Bayesian information criteria test (Kass & Raftery, 1995). However, there are points that lie off the fit that fall into a few higher power signal groups. These groups of points occupy a range of wavelengths from ~110-235 km and two isolated points at ~640±25 km and ~3500±1200 km.

To check for any features that might correlate with the high-power outlying wavelengths, we can use the Fourier transformation to filter to just those wavelengths and compare the resulting filtered topography to geological maps of the BV region. This will allow us to see if a clear pattern of features correlates with the outlying power spectra values. For the first set of wavelengths (~110-235

km), we find that the filtered topography corresponds to deformation belts common across the lowlands of Venus (Young & Hansen, 2007). The range observed in the first set of wavelengths might be a result of the variability in the size of deformation belts in addition to how the sinuous BV intersects the features. Young and Hansen (2007) found that the deformation belts in Rusalka Planitia range from 400 to 2000 km long and 50 to 200 km wide. Our shorter set of wavelength overlaps this range in either case and suggests that the limited horizontal movement that drives the creation of these deformation belts happened since BV formation.

In the middle of our three outlying wavelengths is a point with a wavelength of 640±25 km. This wavelength does not clearly correspond to any source feature along the length of BV. While the spacing of deformation belts could explain this wavelength, an investigation of that spacing showed that along the profile of BV they vary from ~500 to ~900 km, so one would not expect a single peak in the power spectrum. One possibility is that we are seeing the characteristic deformation wavelength of the elastic lithosphere (i.e., the flexural parameter). However, if we apply the equations that allow us to determine the thickness of the elastic lithosphere from the flexural parameter (Turcotte & Schubert, 2014, equation 3.127; parameter values from McGovern et al., 2013), we obtain a value of ~275 km. This is above the global range that varies between 10 km and 50 km (i.e., Brown & Grimm, 1996; McKenzie & Nimmo, 1997; McGovern et al., 2013). The high value we obtain implies that this wavelength is not the flexural parameter. At present we do not have an explanation for this feature, and it may simply be a statistical outlier.

The longest wavelength outlying point in our power spectrum is at ~3500±600 km, with the large uncertainty arising from how the discrete Fourier transform is calculated. While this wavelength does not clearly correspond with any individual feature in our filtered topography for BV, it is comparable to the thickness of Venus's mantle. Since convection-driven dynamic uplift typically has a wavelength comparable to the thickness of the convecting layer (Weller & Kiefer, 2020), this observation suggests that dynamic uplift may be playing a role (cf. Jindal et al., 2018). While the timing of dynamic uplift and convection must post-date BV's formation in the northern canale source location, this does not hold if the source is to the south. In that case, the timing cannot be constrained, although the feature is still observable in the power spectrum. This conclusion is consistent with the long-wavelength correlation between gravity and topography on Venus, again suggesting an important role for convection (e.g., McKenzie 1994).

4. Conclusion

While Baltis Vallis has been deformed and uplifted to the point that little information remains of its original topographic profile, this same feature allows us to investigate post-emplacement processes. We first showed that, depending on BV's emplacement direction, the initial topographic information of BV was modified over most observable wavelengths. This is especially true in the

northern source case, where we show that processes longer than the profile itself (~7000 km in length) must have occurred since the formation of BV. The metric analysis shows that BV represents a system that was emplaced and then experienced tectonic evolution without an ability to evolve concurrently. The outlier topographic power spectra data points represent the characteristic wavelengths of tectonic or dynamic processes that have shifted, tilted, and buckled BV's topographic profile after the canale's emplacement. The characteristic wavelengths that we found give evidence towards processes that are thought to be pervasive across Venus, notably deformation belts and convective uplift. The characteristic wavelengths determined by this study can be used by modelers to help constrain and validate their model results.

This study has potential to be tested and expanded by data from the future *VERITAS* mission to Venus. Much of our analysis is based upon radar imagery and topography derived from the *Magellan* spacecraft. A higher resolution, more complete set of images along the profile of BV could help constrain the source location to a specific volcanic vent or find locations along the canale that imply a flow direction. Crucially, this would resolve the issue of whether the convective uplift post-dated BV emplacement (northern source) or could have pre-dated it (southern source). Beyond the northern (184.6° E, 47.6° N) and southern (166.9° E, 11.5° N) ends of BV, images of specific areas with higher resolution/different incidence perspectives would provide insight. These areas include segments that are proposed to experience avulsion (e.g., 160.9° E, 40.7° N, Stewart & Head, 1999) and a possible lemniscate loop at 160.75° E, 42.12° N (Komar, 1984). Higher resolution topography would also improve the topographic power spectra analysis. While this is unlikely to change the approximate values of our currently observed characteristic wavelengths, it might let us determine characteristic wavelengths for shorter features like wrinkle ridges. Reassessing various features and aspects of Venus' geology in anticipation of future mission results is currently a subject of much interest. Baltis Vallis is particularly interesting in this regard because of its large lateral extent, which we have argued provides clues to the surface and internal evolution of Venus. Future studies of the feature could try to investigate the time evolution of mantle dynamic uplift by comparing model results with the observed topographic characteristics of BV.

Acknowledgements

J. W. Conrad is supported through the NASA Postdoctoral Program Fellowship.

Open Research

Magellan data used in this study are publicly available through the Planetary Data System (radar images used in Figure 1: https://astrogeology.usgs.gov/search/map/Venus/Magellan/Venus
topography: https://astrogeology.usgs.gov/search/map/Venus/Magellan/RadarProperties/Venus_Magellan_
Wieczorek, M. A. (2015)'s Venus topography coefficients are sourced from their Zenodo repository (https://doi.org/10.5281/zenodo.997406).

References

Araki, H., Tazawa, S., Noda, H., Ishihara, Y., Goossens, S., Sasaki, S., Kawano, N., Kamiya, I., Otake, H., Oberst, J., & Shum, C. (2009). Lunar Global Shape and Polar Topography Derived from Kaguya-LALT Laser Altimetry. *Science*, *323*(5916), 897–900. https://doi.org/10.1126/science.1164146

Baker, V. R., Komatsu, G., Parker, T. J., Gulick, V. C., Kargel, J. S., & Lewis, J. S. (1992). Channels and valleys on Venus: Preliminary analysis of Magellan data. *Journal of Geophysical Research: Planets*, *97*(E8), 13421–13444. https://doi.org/10.1029/92JE00927

Bills, B. G., & Kobrick, M. (1985). Venus topography: A harmonic analysis. *Journal of Geophysical Research: Solid Earth*, *90*(B1), 827–836. https://doi.org/10.1029/JB090iB01p00827

Black, B. A., Perron, J. T., Hemingway, D., Bailey, E., Nimmo, F., & Zebker, H. (2017). Global drainage patterns and the origins of topographic relief on Earth, Mars, and Titan. *Science*, *356*(6339), 727–731. https://doi.org/10.1126/science.aag0171

Brown, C. D., & Grimm, R. E. (1996). Lithospheric rheology and flexure at Artemis Chasma, Venus. *Journal of Geophysical Research: Planets*, *101*(E5), 12697–12708. https://doi.org/10.1029/96JE00834

Conrad, J. W., Nimmo, F., Beyer, R. A., Bierson, C. J., & Schenk, P. M. (2021). Heat Flux Constraints From Variance Spectra of Pluto and Charon Using Limb Profile Topography. *Journal of Geophysical Research: Planets*, *126*(2), e2020JE006641. https://doi.org/10.1029/2020JE006641

Ermakov, A. I., Park, R. S., & Bills, B. G. (2018). Power Laws of Topography and Gravity Spectra of the Solar System Bodies. *Journal of Geophysical Research: Planets*, *123*(8), 2038–2064. https://doi.org/10.1029/2018JE005562

Ford, P. G., & Pettengill, G. H. (1992). Venus topography and kilometer-scale slopes. *Journal of Geophysical Research: Planets*, *97*(E8), 13103–13114. https://doi.org/10.1029/92JE01085

James, P. B., Zuber, M. T., & Phillips, R. J. (2013). Crustal thickness and support of topography on Venus. *Journal of Geophysical Research: Planets*, *118*(4), 859–875. https://doi.org/10.1029/2012JE004237

Jindal, A., Hayes, A., & Loredo, T. (2018). *Unveiling the Interior of Venus: Using tectonic deformations along canali to constrain lithospheric structure & mantle convection*. *42*, B4.1-46-18.

Jones, A. P., & Pickering, K. T. (2003). Evidence for aqueous fluid–sediment transport and erosional processes on Venus. *Journal of the Geological Society*, *160*(2), 319–327. https://doi.org/10.1144/0016-764902-111

Kargel, J. S., Kirk, R. L., Fegley, B., & Treiman, A. H. (1994). Carbonate-Sulfate Volcanism on Venus? *Icarus*, *112*(1), 219–252. https://doi.org/10.1006/icar.1994.1179

Kass, R. E., & Raftery, A. E. (1995). Bayes Factors. *Journal of the American Statistical Association*, *90*(430), 773–795. https://doi.org/10.1080/01621459.1995.10476572

Khawja, S., Ernst, R. E., Samson, C., Byrne, P. K., Ghail, R. C., & MacLellan, L. M. (2020). Tesserae on Venus may preserve evidence of fluvial erosion. *Nature Communications*, *11*(1), 5789. https://doi.org/10.1038/s41467-020-19336-1

Komar, P. D. (1984). The Lemniscate Loop: Comparisons with the Shapes of Streamlined Landforms. *The Journal of Geology*, *92*(2), 133–145. https://doi.org/10.1086/628844

Komatsu, G., & Baker, V. R. (1994). Plains Tectonism on Venus: Inferences from Canali Longitudinal Profiles. *Icarus*, *110*(2), 275–286. https://doi.org/10.1006/icar.1994.1121

McGovern, P. J., Rumpf, M. E., & Zimbelman, J. R. (2013). The influence of lithospheric flexure on magma ascent at large volcanoes on Venus. *Journal of Geophysical Research: Planets*, *118*(11), 2423–2437. https://doi.org/10.1002/2013JE004455

McKenzie, D. (1994). The Relationship between Topography and Gravity on Earth and Venus. *Icarus*, *112*(1), 55–88. https://doi.org/10.1006/icar.1994.1170

McKenzie, D., & Nimmo, F. (1997). Elastic Thickness Estimates for Venus from Line of Sight Accelerations. *Icarus*, *130*(1), 198–216. https://doi.org/10.1006/icar.1997.5770

Nimmo, F., Bills, B. G., Thomas, P. C., & Asmar, S. W. (2010). Geophysical implications of the long-wavelength topography of Rhea. *Journal of Geophysical Research: Planets*, *115*(E10). https://doi.org/10.1029/2010JE003604

Oshigami, S., & Namiki, N. (2007). Cross-sectional profiles of Baltis Vallis channel on Venus: Reconstructions from Magellan SAR brightness data. *Icarus*, *190*(1), 1–14. https://doi.org/10.1016/j.icarus.2007.03.011

Press, W. H. (1992). *Numerical Recipes in Fortran 77: The Art of Scientific Computing*. Cambridge University Press. http://lib.pyu.edu.vn/handle/123456789/7588

Sharpton, V. L., & Head III, J. W. (1986). A comparison of the regional slope characteristics of Venus and Earth: Implications for geologic processes on Venus. *Journal of Geophysical Research: Solid Earth*, *91*(B7), 7545–7554. https://doi.org/10.1029/JB091iB07p07545

Shepard, M. K., Campbell, B. A., Bulmer, M. H., Farr, T. G., Gaddis, L. R., & Plaut, J. J. (2001). The roughness of natural terrain: A planetary and remote sensing perspective. *Journal of Geophysical Research: Planets*, *106*(E12), 32777–32795. https://doi.org/10.1029/2000JE001429

Stewart, E. M., & Head, J. W. (1999). *Stratigraphic Relations and Regional Slopes in the Baltis Vallis Region, Venus: Implications for the Evolution of Topography*. 1173.

Turcotte, D., & Schubert, G. (2014). *Geodynamics*. Cambridge University Press.

Weller, M. B., & Kiefer, W. S. (2020). The Physics of Changing Tectonic Regimes: Implications for the Temporal Evolution of Mantle Convection and the Thermal History of Venus. *Journal of Geophysical Research: Planets*, *125*(1), e2019JE005960. https://doi.org/10.1029/2019JE005960

Wieczorek, M. A. (2015). 10.05—Gravity and Topography of the Terrestrial Planets. In G. Schubert (Ed.), *Treatise on Geophysics (Second Edition)* (pp. 153–193). Elsevier. https://doi.org/10.1016/B978-0-444-53802-4.00169-X

Young, D. A., & Hansen, V. L. (2005). Poludnista Dorsa, Venus: History and context of a deformation belt. *Journal of Geophysical Research: Planets*, *110*(E3). https://doi.org/10.1029/2004JE002280